BINARY SYSTEMS WITH APOGEE: HIGHER-ORDER SYSTEMS IN THE SOLAR NEIGHBORHOOD

Hannah M. Lewis
Department of Astronomy, University of Virginia, Charlottesville, VA 22904
Advisor: Steven R. Majewski

Abstract

We present the results of an assessment of hierarchical systems for main-sequence stars within 200 pc of the Sun, utilizing the APOGEE – *Gaia* Wide Binary Catalog. The catalog of 36 wide binary companions were selected by matching *Gaia* parallaxes and proper motions, and confirmed to be gravitationally-bound pairs using APOGEE radial velocities. We identify triple and higher-order multiple candidates using (1) the *Gaia* binary sequence and (2) observed radial velocity variations in APOGEE measurements. Further, we compare abundance differences between the components of the wide binaries and triple- or quadruple- systems, to identify the influence of additional stellar or sub-stellar companions on the assumed identical chemistry of these co-eval pairs.

1. Introduction

Wide binaries are gravitationally bound pairs of stars separated by up to ~ 1 parsec. Formation scenarios for such systems imply that wide binaries are all born at (roughly) the same time and from material of nearly identical chemical makeup. The overall consistency in the metallicity of wide binaries has been studied in detail for a handful of systems (e.g., Gratton et al., 2001), and a few studies have gone beyond metallicity to study individual elements, including Fe (Desidera et al., 2004, 2006), V (Desidera et al., 2006), and Li (Martín et al., 2002).

In a recent study, we compare the chemical abundances of 14 separate elements of dwarf stars in wide binaries to test the abundance consistency of stars of a common origin (Andrews et al., 2019). The sample of 62 stars in 31 wide binaries is identified from a catalog produced by cross-matching Apache Point Observatory Galactic Evolution Experiment (APOGEE; Majewski et al., 2017) stars with US Naval Observatory CCD Astrograph Catalog (UCAC5; Zacharias et al., 2017) astrometry, and we confirm the fidelity of the sample with parallaxes from *Gaia*. We find that the consistency of individual elements (including Fe, Si, K, Ca, Mn, and Ni) between components of the wide binaries is too similar to have anything other than a common origin.

However, other processes may cause abundance differences in wide binaries; in particular, differences in planet formation or accretion in two otherwise identical stars may leave signatures in chemical abundances (Oh et al., 2018). Giant planets have been shown to form more readily around more metal-rich stars (e.g., Fischer & Valenti, 2005) and the elemental abundances of wide binaries that host planets have been studied in detail (e.g., Teske et al., 2016). These studies find significant differences in the abundance patterns, which has been attributed to the fact that forming more gas giants or rocky planets leads to an overall depletion of metals in the gas that will eventually accrete onto the host star (Biazzo et al., 2015; Ramírez et al., 2015).

Utilizing precise radial velocity measurements from the Sloan Digital Sky Survey (SDSS-IV; Blanton et al., 2017) Apache Point Observatory Galactic Evolution Experiment

APOGEE spectroscopic survey for stars in 36 wide binaries, this work aims to identify triple and higher-order multiple candidates and to explore the potential chemical effects of exoplanet formation.

2. Observations and Data

The sample is selected from the wide binary catalog described in El-Badry et al. (2018), which was constructed by searching *Gaia* DR2 for pairs of stars within 200 pc of the Sun, with positions, proper motions, and parallaxes consistent with being gravitationally bound. The El-Badry et al. (2018) catalog contains $> 50,000$ wide binaries, containing main-sequence (MS) and white dwarf (WD) components, with separations of $50 \lesssim s < 50,000$ AU. The catalog provides measurements of proper motion, parallax, magnitude, radial velocity (where measured), and their associated errors, for each star in the pair from *Gaia* as well as the physical separation of the pair and the binary class (i.e., MS/MS, MS/WD, or WD/WD).

The Apache Point Observatory Galaxy Evolution Experiment (APOGEE-2) is a high-resolution ($R \sim 22,500$), high-S/N ($\mathrm{S/N} > 100$), infrared (1.51 μm to 1.69 μm), spectroscopic survey using the 2.5-m Sloan telescope in the Northern Hemisphere and the du Pont telescope at Las Campanas Observatory in the Southern Hemisphere (Majewski et al., 2017). The latest APOGEE-2 data release comprises spectra for ∼398,000 stars, along with stellar parameters ($T_{\rm eff}$, $\log g$, metallicity $[\mathrm{M/H}]$, $[\alpha/\mathrm{M}]$, etc.) and individual chemical abundances for more than a dozen elements, derived from the APOGEE Stellar Parameter and Chemical Abundance Pipeline (ASPCAP; García Pérez et al., 2016). In addition to elemental abundances, APOGEE provides multi-epoch radial velocity (RV) measurements, with a typical precision better than ∼0.1 $\mathrm{km\,s^{-1}}$.

The two catalogs were then cross-matched, adopting a 1” positional tolerance. The APOGEE sample is made up of red giants stars (∼70%) and MS stars (∼30%); stellar remnants (i.e., WDs) are too faint to be observed in the ∼1 hr APOGEE visits. For this reason, the cross-match of the two catalogs contains only MS/MS wide binary pairs. To separate main sequence stars and white dwarfs, El-Badry et al. (2018) required both stars to have a measured *Gaia* $\mathrm{G_{BP}}$-$\mathrm{G_{RP}}$ color, and to have well-resolved photometry. As a consequence of these requirements, the El-Badry et al. (2018) catalog has an effective resolution limit of ∼ 2 arcsec, which is equivalent to the separation limit of APOGEE fibers, which are 2 arsec in diameter. The resulting catalog therefore contains only those wide binaries for which we have APOGEE spectra (as well as good stellar parameters and abundances) for both components of the binary, as well as high-quality astrometry and photometry from *Gaia*.

RVs were not used in the selection of candidate binaries in the El-Badry et al. (2018) catalog, but are a useful check that binaries are gravitationally bound. In genuine binaries, the RVs of the two stars should agree within a few $\mathrm{km\,s^{-1}}$ (within the RV error). For this reason, we require genuine binaries to have APOGEE RVs consistent to within 5 $\mathrm{km\,s^{-1}}$ (i.e., $\Delta\mathrm{RV} \leq 5\,\mathrm{km\,s^{-1}}$). We also select only stars with low median visit RV error, $V_{\rm err,med} \leq 2\,\mathrm{km\,s^{?1}}$, and high $\mathrm{S/N} \geq 25$ to remove stars with low-quality spectra causing errors in the derived parameters and RVs. These cuts ensure minimum contamination of the wide binary sample by random alignments.

We also remove stars flagged with the ASPCAPFLAGS STAR_BAD or NO_ASPCAP_RESULT, and pairs where one or both stars do not have calibrated $[\mathrm{M/H}]$ measurements, to ensure that we are considering only stars with reliably determined stellar parameters and abundances.

The APOGEE – *Gaia* Wide Binary Catalog contains 36 genuine MS/MS wide binaries, shown in $T_{\rm eff}$-$\log g$ in Fig. 1, with separations $300 \lesssim s < 50,000$ AU within 200 pc of the Sun.

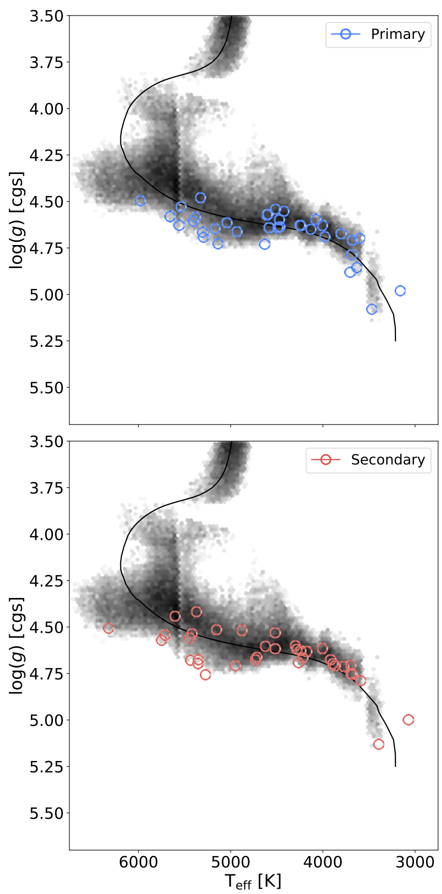

Figure 1: The calibrated $\log g$ and $T_{\rm eff}$ of the components in our binaries, as measured by APOGEE. The gray histogram in the background shows the $\log g$ and $T_{\rm eff}$ of APOGEE stars. A 5 Gyr solar isochrone is shown in black.

APOGEE calibrates its $\log g$ for giant stars to detailed astroseismic models of stars in the Kepler field, while cluster stars and stellar evolution models are used to calibrate other stellar parameters (García Pérez et al., 2016). The latest APOGEE data release includes stellar abundance calibrations for dwarf stars based on open clusters (Holtzman et al., 2018); however, the dwarfs stellar parameters in the APOGEE catalog rely on uncalibrated ASPCAP parameters, which leads to an overestimation in the surface gravity for the coolest dwarf stars; the $\log g$ shown in the figure is, therefore, the calibrated $\log g$, as defined by

$$(\log g)_{\rm cal} = \log g - (1.25\times10^{-4})(T_{\rm eff} - 6400\,{\rm K}), \quad (1)$$

where $\log g$ and $T_{\rm eff}$ are the uncalibrated surface gravity and effective temperature. The equation represents a linear correction applied to dwarf stars to fit the Dartmouth isochrone, shown in Fig. 1 (solid black line).

In addition to stellar parameters, the APOGEE reduction provides RV measurements with precisions typically better than $\sim$0.1 km s^{-1}. The leftmost panel of Fig. 2 compares the APOGEE RVs for the components of the 36 wide binaries that we have identified. The measurement uncertainties are shown, but are small compared to the size of the data points. In the center panel, for the 12 cases where both components of the wide binaries have RVs measured by *Gaia*, a comparison of the *Gaia* RVs are shown. That the data points lie on top of the one-to-one line in both of these plots is expected if the pairs are genuine wide binaries. Finally, the rightmost panel of Fig. 2 shows the difference between the RVs measured by the two surveys – for the 12 pairs where both components of the wide binaries have RVs measured by both surveys – as a function of *Gaia* G magnitude. The RV measurements are in good agreement between the surveys, except for one star which has a relatively low-S/N spectra with APOGEE (G $\sim$ 13 mag, S/N $\sim$ 70).

We compare the *Gaia* proper motions and parallax for the stars in the 36 wide binaries in Fig. 3. Again, measurement uncertainties are smaller than the data points. The clear consistency between the parallaxes and RVs of the stars in these pairs suggests that our sample is free from contamination by random alignments.

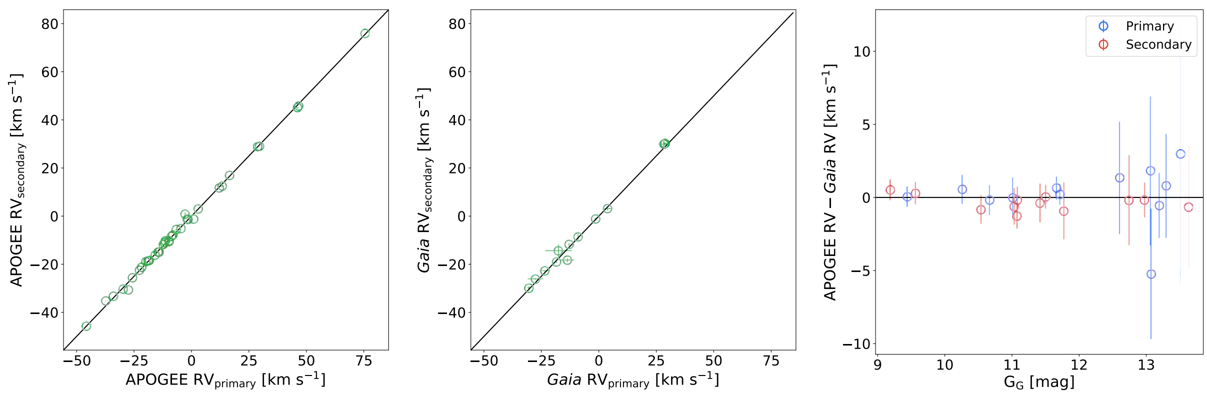

Figure 2: The leftmost plots compare the APOGEE radial velocities for components of the wide binaries, and the *Gaia* radial velocities for the few cases where measurements are available for both binary components. The rightmost panel shows that the binaries in our sample have consistent velocities as measured by the two surveys for the 12 binaries that have RVs measured by *Gaia*.

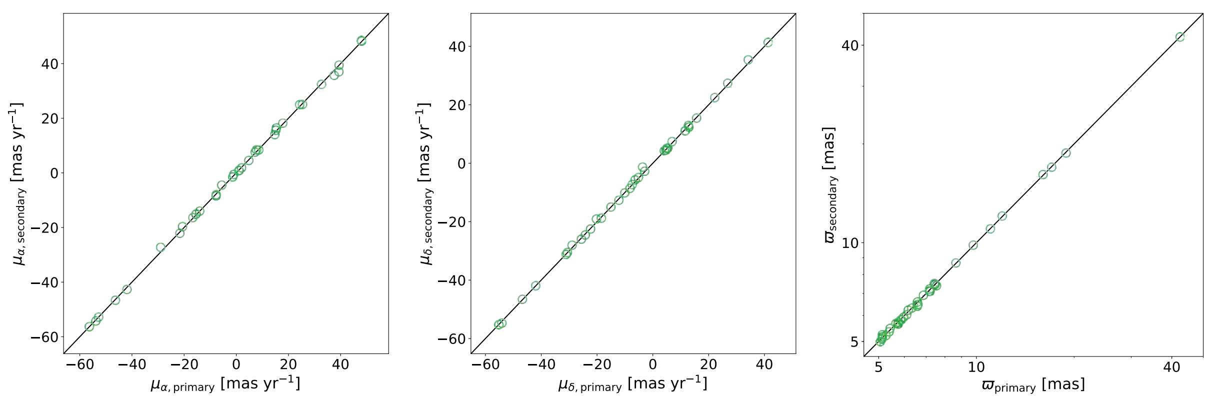

Figure 3: We compare the *Gaia* proper motions in both right ascension (μ_α) and declination (μ_δ) in the left two panels. The third panel shows that the binaries in our sample have consistent parallaxes, as measured by *Gaia* for the 36 binaries that are measured by *Gaia*.

3. Results

In this section we outline the multiple methods utilized to detect candidate companions in these wide binary systems, and report all candidate companions.

A. Binary Sequence

An unresolved binary system comprising two identical stars has the same color but twice the luminosity of an equivalent single star; such a system, comprising two equal-mass main-sequence stars, will appear in the color-magnitude diagram 0.753 mag brighter, irrespective of the wavelength bands used. We show in Fig. 4 the *Gaia* G_{BP}-G_{RP} color against the absolute *Gaia* G magnitude. The grey histogram in the background shows the density of stars from the cross-match of APOGEE with the full *Gaia* DR2 catalog, including MS and giant stars. We overplot a 5 Gyr, solar-metallicity Dartmouth isochrone (solid black line), as well as the corresponding binary MS, shifted 0.753 mag in absolute magnitude.

The figure confirms that all of the stars in our sample are on the main sequence, and identifies four components of four separate

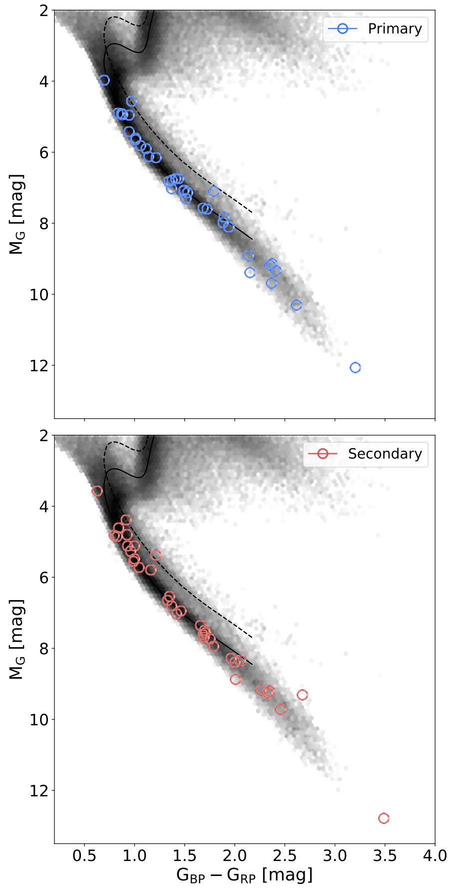

Figure 4: The *Gaia*-based color-magnitude diagram. The grey histogram in the background shows the density of stars from the cross-match of APOGEE with the full *Gaia* DR2 catalog. In each binary, the "primary" is the object with the larger photometrically-inferred mass, as derived by El-Badry et al. (2018).

wide binaries which lie on the binary sequence.

B. Radial Velocity

An APOGEE "visit" is defined as the combined spectrum of a source from a single night's observations ($\sim 1\,$hr of exposure). The total survey number of visits scheduled for a star depends on its H mag, with fainter targets requiring more visits to obtain the accumulated S/N of 100; at the completion of the survey, all stars are expected to have a minimum of 3 visits to accomplish this goal. Though the APOGEE survey is not complete at the time of publication of this paper, all of the stars in the APOGEE – *Gaia* Wide Binary Catalog are brighter than $\sim 12.5\,$mag in H, and so have high-S/N combined spectra, though they may have < 3 visit spectra.

i. Orbit Fitting

APOGEE RVs reach a typical precision $\lesssim 100\,\mathrm{m\,s^{-1}}$, which is sufficient for the detection of RV oscillations expected from relatively short-period companions down to a few Jupiter-masses ($10^{-3}\,\mathrm{M_\odot}$). In this work, we adopt $2\,\mathrm{M_{Jup}}$ as our lower detection limit. For stars with ≥ 8 visits, over a sufficient temporal baseline (i.e., longer than the period of the orbit), these high-quality RV measurements are suitable to not only detect RV variability, but also to derive Keplerian orbital fits.

For stars with fewer RV measurements, there are many stellar- or exoplanet-mass companion orbit models that are consistent with the data, which leads to a challenging search to sample over all possible orbital parameters. *The Joker* (Price-Whelan et al., 2017) provides a Monte Carlo sampler, intended for systems with sparse RV measurements, that produces correct samplings in orbital parameters for data that include as few as 3 visits; however, for ≤ 5 visits, the returned samples are highly multimodal, with the samples tending to form a harmonic series for systems 3 RV measurements. For this reason, we limit our orbit fitting using *The Joker* to those stars in the wide binary catalog with 6 or more RV measurements with APOGEE. In the APOGEE – *Gaia* Wide Binary Catalog 16 stars in 10 wide binary pairs have ≥ 6 visits, and so are eligible for Keplerian orbit fitting with *The Joker*.

Orbit fitting with *The Joker* was performed for all stars with ≥ 6 RV measurements with APOGEE, and all candidate heirarchical systems are reported here. Note, we do not report here systems for which *The Joker* returned highly multi-modal samples; we only report those systems with a unimodal, unique solution. One example – out of the six sub-stellar mass companion candidates detected in the sample – is shown in Fig. 5.

ii. Minimum Mass Estimation

Of the remaining stars (with $\leq$ 5 visits), $\sim$ 10% have more than 3 visits, and a majority ($\sim$ 60%) have 2 to 3 visits. To characterize these very sparsely sampled systems, we use the difference between the highest and lowest measured RVs for each star, $\Delta\mathrm{RV}_{\mathrm{max}} = \max(\mathrm{RV}_n) - \min(\mathrm{RV}_n)$ (Badenes et al., 2012; Maoz et al., 2012; Badenes et al., 2018). We will use $\Delta\mathrm{RV}_{\mathrm{max}}$ as a proxy for the minimum peak-to-peak amplitude, $\Delta\mathrm{RV}_{\mathrm{p-p}}$, of the system's RV curve, in order to derive a lower-limit to the mass of the candidate companion. In order to derive this lower-limit, we will assume (1) the peak-to-peak amplitude of the RV curve, $\Delta\mathrm{RV}_{\mathrm{max}} = \Delta\mathrm{RV}_{\mathrm{p-p}}$, is twice the semi-amplitude, K, of the orbit, (2) all companion orbits are circular (eccentricity $e = 0$), and (3) all companions orbit at the critical period for Roche Lobe overflow.

The critical period is defined as

$$P_{\mathrm{crit}} = 2\pi\mathcal{R}(q)\sqrt{\frac{R_*^3}{GM_*}} \tag{2}$$

where $\mathcal{R}(q)$ is the ration between the radius of the Roche Lobe and the orbital separation, which can be approximated as 0.30, the average over the range $0 < q < 1$ (Eggleton, 1098), and M_* and R_* are the mass and radius of the star, derived via the Torres et al. (2010) relations.

For the companions at the critical period, the peak-to-peak amplitude of the RV curve, $\Delta\mathrm{RV}_{\mathrm{p-p}}$, is twice the semi-amplitude, K, such that

$$\Delta\mathrm{RV}_{\mathrm{p-p}} = 2K = 2\left(\frac{\pi G M_f}{2P_{\mathrm{crit}}}\right)^{1/3}, \tag{3}$$

where M_f is the mass function, $M_f = (m\sin i)^3/(M_* + m)^2$. The variable of interest then, for detecting candidate companions in systems with sparsely sampled RV curves is

$$M_f = \frac{(m\sin i)^3}{(M_* + m)^2} = \frac{P_{\mathrm{crit}}}{2\pi G}\left(\frac{\Delta\mathrm{RV}_{\mathrm{p-p}}}{2}\right)^3. \tag{4}$$

We solve the above equation iteratively, to derive the minimum companion mass; we solve the equation for the $\sin i = 1$ case, and thus use $m \approx m\sin i$ after the first iteration.

For all stars in the APOGEE – *Gaia* Wide Binary Catalog with insufficient visits for Keplerian orbit fitting, we derive the minimum companion mass $m\sin i$. We detect two additional sub-stellar mass companion candidates (which had not already been detected via the orbit fitting method); one of these candidates orbits the secondary star in a wide binary system where the primary also has a companion detected via orbit fitting.

4. Conclusion

From the sample of 36 pairs in the APOGEE – *Gaia* Wide Binary Catalog, in total, we identify 4 stellar mass companions in 4 wide binary systems, and 8 sub-stellar (minimum) mass companion candidates in 7 systems, resulting in 10 detected triples and 1 quadruple system.

In a preliminary analysis of the metallicities of these stars, we confirm the planet-metallicity correlation (i.e., higher metallicity stars are more likely to host planets Fischer & Valenti, 2005), as shown in Fig. 6 (upper panel). We also compare the metallicity differences, normalized to the measurement uncertainties, of our wide binary sample for both companion hosting systems and for systems where no companion (sub-stellar or stellar mass) is detected. The systems which host detected companions appear to have smaller discrepancies in metallicity (middle panel of Fig. 6), which is unexpected; however, this is likely a detection effect, not an astrophysical one. Systems

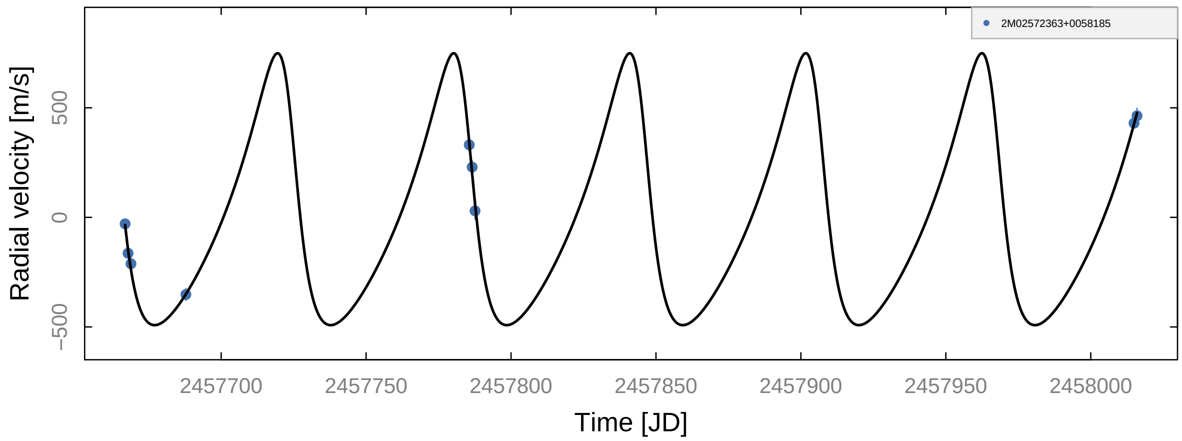

Figure 5: Radial velocities of an RV variable star in the APOGEE – *Gaia* Wide Binary Catalog. The measured RVs are shown in blue, and the best-fit RV curve is shown in black. The companion candidate has a period of 60.7 days and mass $\gtrsim 11.7\,\mathrm{M_{Jup}}$.

for which we are able to detect companions via the RV methods described in this work require multiple APOGEE visits; these systems therefore have higher-S/N, which in-turn means they have more accurately measured values for [M/H], with similar levels of uncertainty, so the value $\Delta[\mathrm{M/H}]/\sigma$ is lower for the sample of candidate companion hosts (shown in the bottom panel of Fig. 6). Similar analysis for the 14 elements reliably measured by APOGEE for dwarf stars (C I, O, Mg, Al, Si, P, S, K, Ca, Ti, V, Mn, Fe, and Ni, Andrews et al., 2019) for a large fraction of the wide binary components is forthcoming.

Acknowledgments

This research has made use of the Tool for OPerations on Catalogues And Tables (TOPCAT; Taylor, 2005). This work was aided by VSGC funding, as well as funding from the National Science Foundation and the Jefferson Scholars Foundation.

Funding for the Sloan Digital Sky Survey IV has been provided by the Alfred P. Sloan Foundation, the U.S. Department of Energy Office of Science, and the Participating Institutions. SDSS-IV acknowledges support and resources from the Center for High-Performance Computing at the University of Utah. The SDSS web site is www.sdss.org.

References

Abolfathi, B., Aguado, D. S., Aguilar, G., et al. 2018, *ApJS*, 235, 42

Andrews, J. J., Chanamé, J., & Agüeros, M. A. 2017, *MNRAS*, 472, 675

Andrews, J. J., Anguiano, B., Chanamé, J., et al. 2019, *ApJ*, 871, 42

Badenes, C., & Maoz, D. 2012, *ApJ*, 749, 11

Badenes, C., Mazzola, C., Thompson, T. A., et al. 2018, *ApJ*, 854, 147

Biazzo, K., Gratton, R., Desidera, S., et al. 2015, *A&A*, 583, 135

Blanton, M. R., Bershady, M. A., Abolfathi, B., et al. 2017, arXiv:1703.00052

Desidera, S., Gratton, R. G., Scuderi, S., et al. 2004, *A&A*, 420, 683

Desidera, S., Gratton, R. G., Lucatello, S., et al. 2006, *A&A*, 454, 581

Eggleton, P. P. 1983, *ApJ*, 268, 368

El-Badry, K., & Rix, H. W. 2018, *MNRAS*, 480, 4884

Fischer, D. S., & Valenti J. 2005, *ApJ*, 662, 1102

García Pérez, A. E., Allende Prieto, C., Holtzman, J. A., et al. 2016, *AJ*, 151, 144

Gratton, R. G., Bonanno, G., Claudi, R. U., et al. 2001, *A&A*, 377, 123

Holtzman, J. A., Hasselquist, S., Shetrone, M., et al. 2018, *AJ*, 156, 125

Mack, III, C. E.., Schuler, S. C., Stassun, K .G., et al. 2014, *ApJ*, 787, 98

Majewski, S. R., Schiavon, R. P., Frinchaboy, P. M., et al. 2017, AJ, 154, 94

Maoz, D., Badenes, C., & Bickerton, S. J., 2012, *ApJ*, 751, 143

Martín, E. L., Basri, G., Pavlenko, Y., et al. 2002, *ApJ*, 597, 437

Oh, S., Price-Whelan, A. M., Brewer, J. M., et al. 2018, *ApJ*, 854, 138

Price-Whelan, A. M., Hogg, D. W., Foreman-Mackey, D., et al. 2017, *ApJ*, 837, 20

Price-Whelan, A. M., Hogg, D. W., Rix, H. W., et al. 2018, *AJ*, 156, 18

Ramírez, I., Khanal, S., Aleo, P., et al. 2015, *ApJ*, 808, 13

Taylor, M. B. 2005, *ASPC*, 347, 29

Teske, J. K., Shectman, S. A., Vogt, S. S., et al. 2016, *AJ* 152, 167

Torres, G., Andersen, J., & Giménez, A., 2010, *A&AR*, 18, 67

Troup, N., Nidever, D. L., Lee, N. D., et al. 2016, *AJ* 151, 85

Zacharias, N., Finch, C., Frouard, J., et al. 2017, *AJ* 153, 166

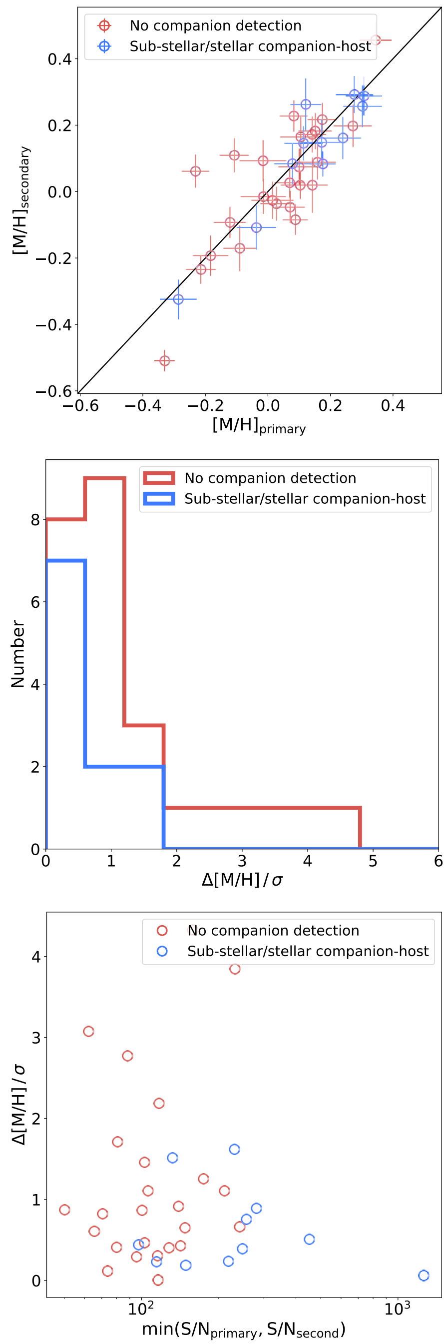

Figure 6: We compare the overall metallicity of each star in our wide-binary sample, as measured by APOGEE. The plot shows that systems with at least one companion candidate tend to have higher metallicities.